NASA TECHNICAL NOTE

NASA TN D-3534

NASA TN D-3534

ANALYSIS OF PERFORMANCE OF DOUBLE-REFLECTOR SYSTEM FOR COLLECTING SOLAR ENERGY

by Gabriel Kaykaty

Lewis Research Center
Cleveland, Ohio

NATIONAL AERONAUTICS AND SPACE ADMINISTRATION • WASHINGTON, D. C. • JULY 1966

NASA TN D-3534

ANALYSIS OF PERFORMANCE OF DOUBLE-REFLECTOR SYSTEM FOR COLLECTING SOLAR ENERGY

By Gabriel Kaykaty

Lewis Research Center
Cleveland, Ohio

NATIONAL AERONAUTICS AND SPACE ADMINISTRATION

For sale by the Clearinghouse for Federal Scientific and Technical Information
Springfield, Virginia 22151 – Price $2.00

ANALYSIS OF PERFORMANCE OF DOUBLE-REFLECTOR SYSTEM FOR COLLECTING SOLAR ENERGY

by Gabriel Kaykaty

Lewis Research Center

SUMMARY

A double-reflector system for collecting solar energy was analyzed with regard to its performance to provide an appraisal of its applicability to a solar Brayton cycle power system. The maximum efficiency expected under the most favorable conditions was predicted and compared with that of a collection system consisting of a single paraboloid with the receiver aperture at the focus.

The double-reflector collection system which was surveyed employed a paraboloid for a primary reflector, and either an ellipsoid or a hyperboloid for a secondary reflector. The study explored the effects of the primary paraboloidal reflector profile, the secondary reflector profile, the secondary reflector axial displacement, and the receiver aperture position on the collection system efficiency. The surface accuracy of the reflector was represented by an angular error in the plane of the optic axis of 15 minutes maximum on the paraboloid and 6 minutes maximum on the hyperboloid or ellipsoid. The technique for computing the collection system efficiency was to choose a receiver aperture diameter to capture all the energy reflected from the secondary reflector.

A double-reflector collection system with a hyperboloidal secondary reflector will achieve the same maximum efficiency as a system with an ellipsoidal secondary reflector. The efficiency of the double-reflector system is lower than the efficiency of the conventional single-reflector system. For a surface reflectivity of 0.9 and a receiver operating temperature of 2200° R, the maximum collection system efficiency of the double-reflector system is 71 percent compared with a maximum of 81 percent for the single-paraboloidal-reflector system. At the maximum efficiency of the double-reflector system, the projected operating temperature of the secondary reflector is approximately 1100° R. A lower surface reflectivity or a higher receiver operating temperature will exhibit a still greater difference in the efficiency of the two collection systems. In addition, a lower reflectivity will promote a higher secondary reflector operating temperature.

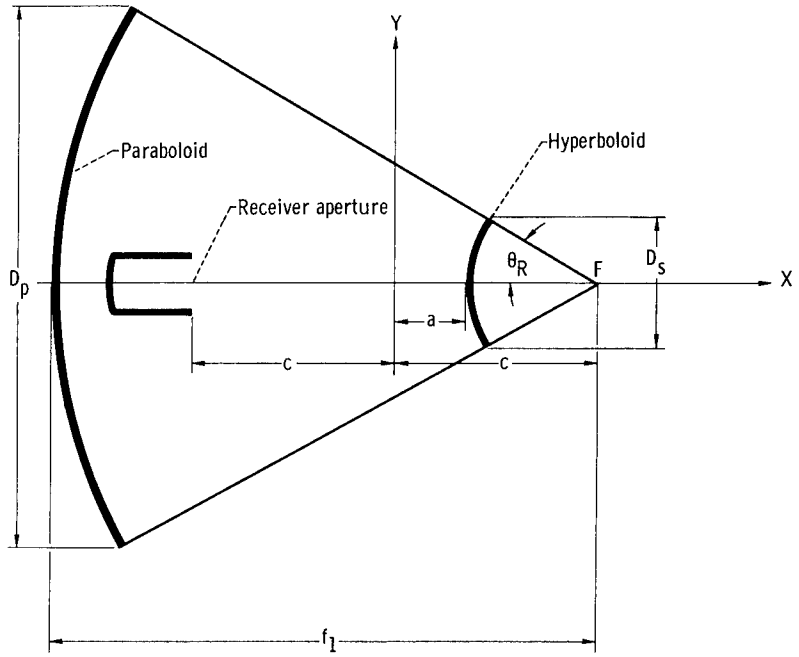

(a) Hyperboloidal.

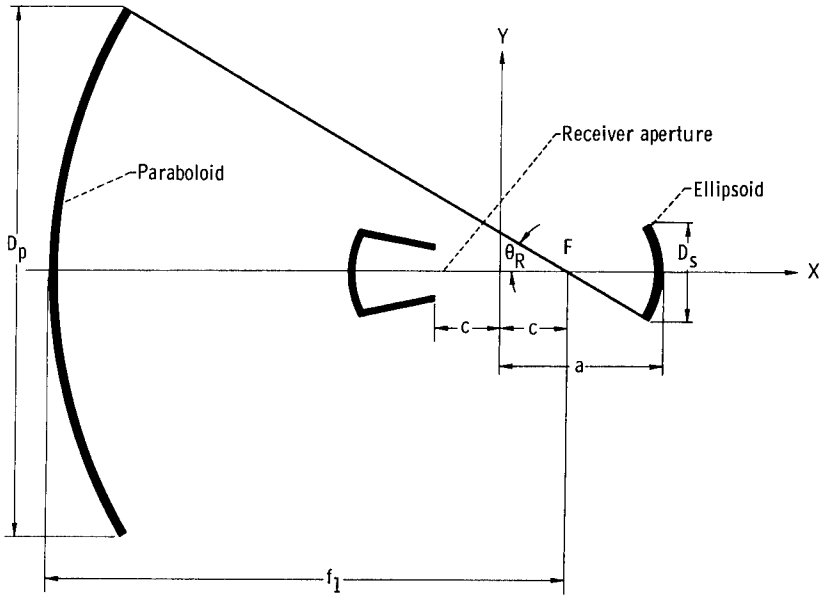

(b) Ellipsoidal.

Figure 1. - Schematic diagrams of double-reflector solar collection systems.

INTRODUCTION

The solar-energy collection system usually considered for a solar dynamic-power generation system utilizes a single paraboloidal reflector. In such a system, the solar rays are reflected from the paraboloidal reflector into a cavity receiver where the energy is used to heat the conversion system working fluid. This configuration may result in significant obstruction loss since the receiver and conversion system, which are usually packaged close together to minimize thermal and pressure losses, are located in front of the reflector. In addition, the requirement for a compact launch configuration may result in a difficult deployment procedure, in which either a large reflector or a rather bulky conversion system must be deployed into its proper relative position.

Another type of collection system is the double-reflector collection system shown in figure 1. This system collects the solar rays on a primary paraboloidal reflector and focuses them at one focus of a hyperboloidal (in a Cassegrainian system) or ellipsoidal (in a Gregorian system) reflector from which they are reflected back to the cavity receiver located at the second focus. Although this system involves an additional reflection which results in some penalty in collection efficiency, it may in some instances offer some improvement over the single-reflector system from the standpoint of either obstruction or packaging and deployment difficulties and may, therefore, be of interest.

The purpose of this study is to evaluate the collection efficiency that may be expected of a double-reflector collection system and compare it with that of a single-paraboloidal-reflector collection system.

A simplified procedure was employed to evaluate the efficiencies of both collection systems. With this procedure, the reflectors are specified by the maximum surface error, and the receiver aperture is sized to capture all the energy reflected from the reflectors rather than to balance increasing receiver radiation losses with increasing energy collection. This approach leads to conservative estimates of the collection system efficiency, but it adequately indicates relative changes in performance as the collection system parameters are varied and permits a comparison of performance between different types of collection systems.

In order to attain higher collection system efficiencies, the energy reflected from the secondary reflector should be concentrated into the smallest area possible, while the diameter of the secondary reflector should be reduced as much as possible. The first condition, which provides a small receiver aperture, will minimize the radiation losses from the receiver; while the second condition will minimize the obstruction losses.

The magnitude of these losses was analyzed by varying the rim angle of the primary paraboloidal reflector, the size and shape of the secondary hyperboloidal and ellipsoidal reflectors, and the separation distance between the focuses of the primary and secondary

reflectors. The maximum collection system efficiency was determined from the results of the analysis.

SYMBOLS

a	distance between vertex of secondary reflector and origin, ft
b	geometric parameter associated with secondary reflector, ft
c	distance between focus of secondary reflector and origin, ft
D_p	diameter of paraboloid, ft
D_r	diameter of paraboloidal reflector subtended by receiver aperture from the focus, ft
D_s	diameter of secondary reflector, ft
D_x	diameter of paraboloidal reflector from which energy is obstructed, ft
d	y-intercept of ray reflected from paraboloid, ft
d_a	y-intercept of ray reflected from paraboloid when the secondary reflector is displaced, ft
E_a	energy absorbed by receiver, Btu/hr
E_i	energy incident in space on projected area of paraboloidal reflector, Btu/hr
E_r	energy lost by receiver, Btu/hr
e	eccentricity of secondary reflector, c/a
F	focus of paraboloid
f_1	focal length of paraboloid, $\frac{D_p(1 + \cos \theta_R)}{4 \sin \theta_R}$, ft
k	distance between focus and point on paraboloid, ft
m_{rp}	slope of ray reflected from paraboloid
m_{th}	slope of tangent to hyperbola
R	radial location of point in plane of receiver aperture, ft
r	radius of receiver aperture, ft

S	space solar constant in vicinity of Earth, 442 Btu/(hr)(ft^2)
T	operating temperature of receiver surface, ^oR
X	optic axis
x, y	coordinates of intersection of ray with secondary reflector
Δx	axial displacement of secondary reflector along optic axis, ft
α	effective absorptivity of receiver for solar radiation
β	subtended half-angle of Sun in vicinity of Earth, min
δ_1	angular deviation of normal to primary reflector surface from ideal, min
δ_2	angular deviation of normal to secondary reflector surface from ideal, min
ϵ	effective emissivity of receiver to thermal radiation
η	efficiency of collection system, percent
θ	angle formed by point on paraboloid and optic axis, as measured from focus of paraboloid, deg
θ_R	rim angle of paraboloid; that is, angle formed by rim of paraboloid and optic axis, measured from focus of paraboloid, deg
ξ	angle of normal to secondary surface measured clockwise from optic axis, deg
ρ	reflectivity of reflectors
σ	Stefan-Boltzmann constant, 1712×10^{-12} Btu/(hr)(ft^2)($^oR^4$)
φ	angle formed by ray reflected from secondary reflector and optic axis, deg
ω	supplement of angle ξ, deg

DESCRIPTION OF DOUBLE-REFLECTOR COLLECTION SYSTEM

The arrangement of a double-reflector collection system, which consists of a pair of reflectors and a cavity receiver where the secondary or smaller reflector is a hyperboloid or an ellipsoid, is illustrated in figure 1 (p. 2). One focus of the secondary reflector is coincident with the focus of the paraboloid, while the conjugate focus is at the center of the receiver aperture. The line through the centers of the reflectors and the receiver is the optic axis. All incident rays of energy parallel to the optic axis will, upon reflection from a double-reflector system of perfect reflectors, converge at the second focus, which represents the location of maximum concentration and is, thereby, the

position at which the receiver aperture is placed.

The distance c is that of each focus of the secondary reflector from its origin, and a is the distance from the vertex of the secondary reflector to its origin. The ratio c/a is the eccentricity e of the secondary reflector. The eccentricity of the hyperboloid is greater than 1, and for the ellipsoid it is between 0 and 1. The values of c and e together are sufficient to specify the contour of the secondary reflector. These quantities combined with the rim angle θ_R are sufficient to designate the diameter of the secondary reflector. The primary or larger reflector, which is the paraboloid, is characterized by its rim angle θ_R and its focal length f_1.

The incident solar radiation being collected is subjected to a reflection by the primary reflector followed by a reflection from the secondary reflector, which directs it through the receiver aperture to be absorbed by the receiver walls. The collection system efficiency is a measure of the net energy retained by the receiver for utilization by an energy conversion cycle after obstruction, reflection, and radiation losses have been charged; it is expressed as a ratio of the net useful energy to the energy incident upon the projected area of the primary reflector.

PROCEDURE

The derivation of the equation for computing the efficiency of a double-reflector collection system is presented in appendix A. The technique employed to calculate the efficiency for both the double-reflector collection system and the single-paraboloidal-reflector system was based on a receiver aperture sized to capture all the energy reflected to the plane of the receiver aperture. In order to size the receiver aperture by this method, a knowledge of the region over which solar energy spreads in the plane of the aperture is required. This region is defined by the location of the ray reflected from an element with maximum angular surface error located at the rim of the primary reflector. A ray-trace technique that follows the path of solar rays from incidence on the paraboloid to interception by the target plane containing the receiver aperture is used to determine the position of the ray.

Appendix B contains the method of locating solar rays reflected by a double-reflector system and the determination of the receiver aperture radius. Use of this simplified technique results in a slightly larger-than-optimum aperture size, and in a slightly lower-than-optimum performance. The optimum aperture would be selected through an analysis of the exchange between increasing radiation losses and increasing amounts of energy entering a receiver as the aperture is increased; this procedure requires a difficult detailed determination of energy distribution in the plane of the receiver aperture. The adopted technique, which eliminates the need for the energy distribution, is quite

adequate for comparative purposes and for determining performance trends.

A computer program was formulated to perform the computation of collection system efficiency for a range of eccentricities, focus sizes, and paraboloidal rim angles. The diameter of the paraboloid D_p was maintained constant, while D_s and r were calculated for the range of the variables. In addition, the effect of an axial displacement Δx in the secondary reflector was explored for the range of values of e, c, and θ_R. The axial displacement Δx measures the dislocation in the position of the secondary collector focus from that of the primary focus along the optic axis. The value of Δx was varied in order to assess the sensitivity of the system performance in regard to the relative positioning of the reflectors. The effect of Δx on the location of a ray reflected from the double-reflector system is presented in appendix D.

The reflector angular surface error, which specifies the angular deviation of the normal to the reflector surface from the ideal, is incorporated in the program to establish the concentrating ability of the collection system. Only the surface error measured in a plane containing the optic axis was considered in this analysis because it has the largest effect on the collection system performance and its use simplifies the analysis. The surface error of the reflectors was designated as a maximum of 15 minutes for the paraboloid and a maximum of 6 minutes for the hyperboloid or ellipsoid. This accuracy is attainable by the present methods of reflector fabrication and status of collection system technology for the respective sizes and shapes.

It was assumed that $\rho = 0.9$ and that the receiver cavity was a blackbody with a surface temperature of 2200° R, which is in keeping with the expected cavity temperature for Brayton cycle receivers currently being investigated. The system was considered to operate in the vicinity of the Earth where the incident solar flux is 130 watts per square foot.

Obstruction losses in a double-reflector collection system can occur from two sources: (1) the secondary reflector, which, by being located in front of the primary reflector, obstructs the incident solar radiation and (2) the receiver and conversion equipment package, which obstructs energy being reflected from the primary to the secondary reflector. As this package is moved closer to the secondary reflector (when 2c is made smaller), this obstruction becomes greater. The extent of this interference is a function of the specific size and arrangement of the combination of the receiver and conversion equipment. To determine the performance of the double-reflector collection system under the most favorable circumstances, the obstruction of energy between the two reflectors is limited to that energy being reflected by the segment of the primary reflector that is subtended by the receiver aperture at the first focus.

The nature of the obstructions and the corresponding portions of the primary reflector affected by each source are shown in figure 2. The obstruction loss factored into the computation of collection system efficiency is either the receiver obstruction loss as

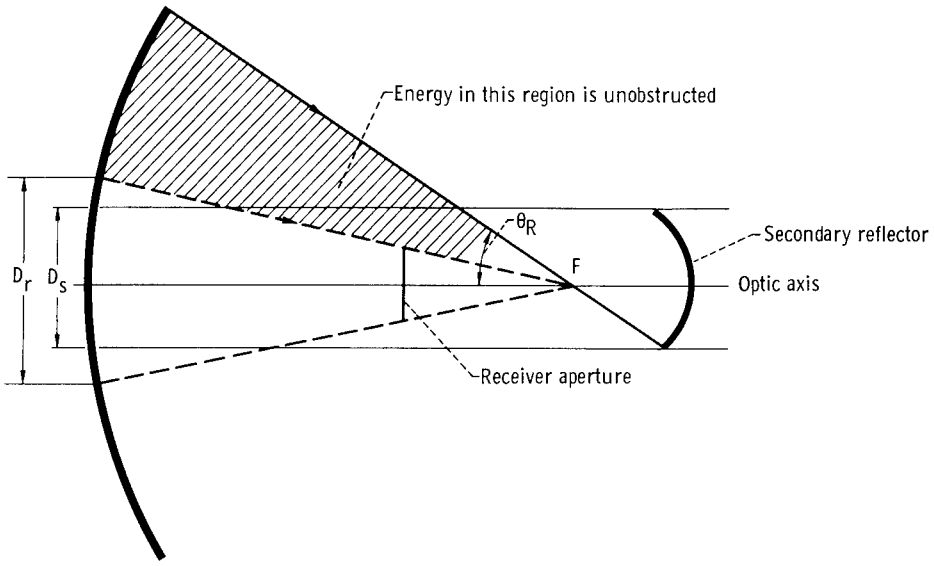

Figure 2. - Sources of obstruction in double-reflector collection system.

dictated by the aperture diameter or the secondary reflector obstruction loss, whichever is larger.

The collection system efficiency was determined for a double-reflector system employing a paraboloidal primary reflector with a rim angle of 60°, 70°, or 80° in conjunction with hyperboloids having eccentricities of 1.2 to 4.0 and ellipsoids having eccentricities of 0.25 to 0.8. The secondary reflector focal point separation 2c expressed as a fraction of the primary reflector focal length $2c/f_1$ was varied from 0.077 to 1.0. The secondary reflector axial displacement Δx expressed as a fraction of the primary reflector focal length $\Delta x/f_1$ was varied from 0 to 0.0045.

RESULTS AND DISCUSSION

Both the collection system efficiency of the double-reflector collection system and the diameters of the secondary reflector were computed on the basis of the stated conditions. A primary reflector diameter of 30 feet, which is roughly the maximum size of a nonfoldable reflector that can be accommodated by a Saturn-5 vehicle, was chosen to illustrate the collection system efficiency. The results are presented in figures 3 to 8. Figures 3 to 5 describe the double-reflector collection system with a hyperboloidal secondary reflector, and figures 6 to 8 describe the double-reflector system with an ellipsoidal secondary reflector.

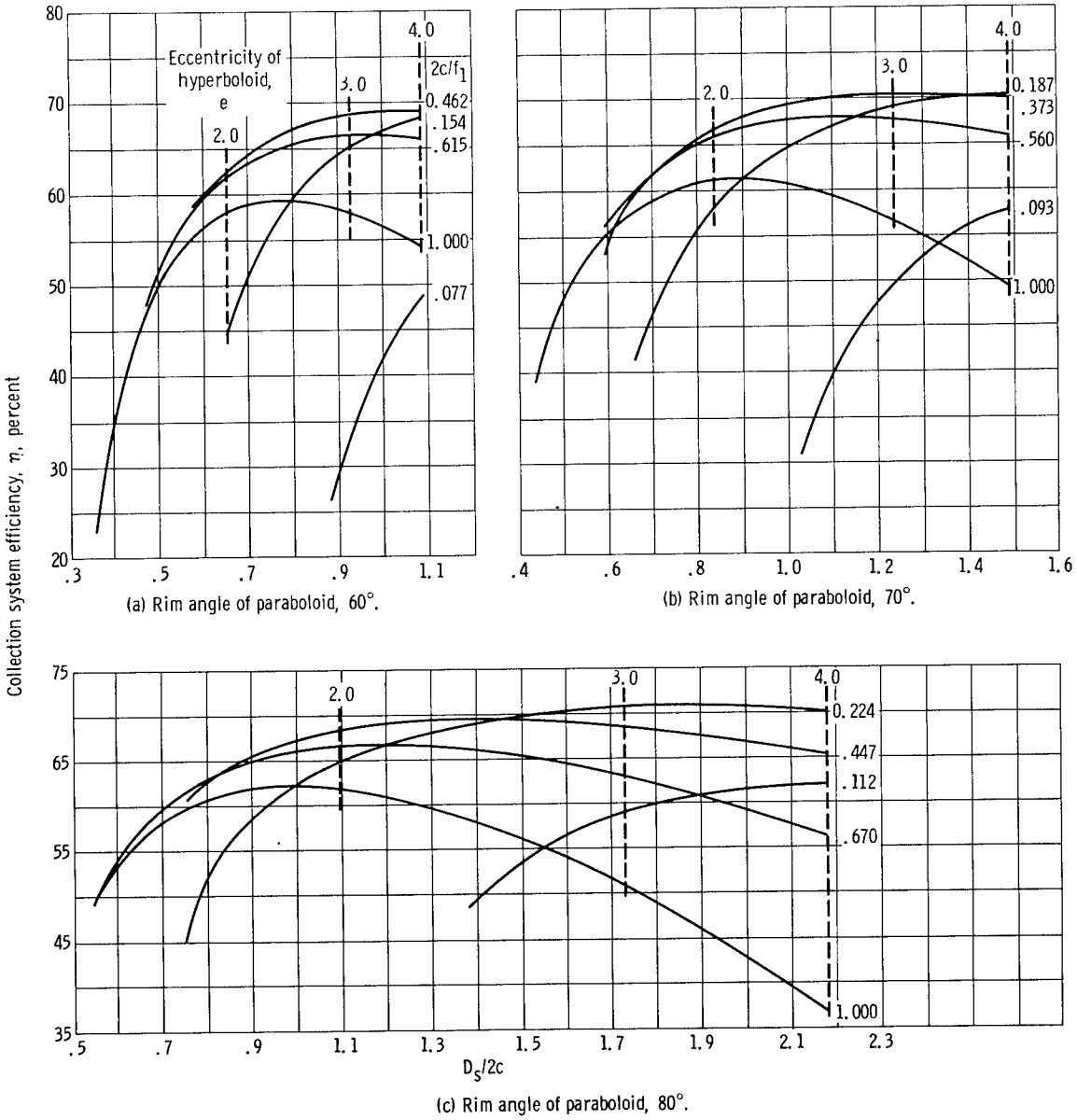

Figure 3. - Effect of hyperboloidal secondary reflector size and contour on efficiency of double-reflector collection system.

Hyperboloidal Secondary Reflector

Figure 3(a) shows the collection system efficiency of the double-reflector system with a hyperboloidal secondary reflector and a 60^{o} paraboloidal primary reflector rim angle as a function of $D_s/2c$ for various values of $2c/f_1$. The ratio $D_s/2c$ is a dimensionless expression for the diameter of the secondary reflector and a measure of its shadowing of the primary reflector. Lines of constant eccentricity are also shown.

For each value of $2c/f_1$, the collection system efficiency increases rapidly with growing values of $D_s/2c$ up to the maximum because of an increasing concentration of energy, which decreases the receiver radiation loss. After the maximum value is reached, the simultaneously increasing obstruction losses of the secondary reflector predominate. Similar trends are noted for paraboloid rim angles of 70^o and 80^o in figures 3(b) and (c).

The peak efficiencies from figure 3 are plotted in figure 4 as functions of $2c/f_1$ for the three paraboloid rim angles. The curves demonstrate that the peak collection system efficiency increases with decreasing values of $2c/f_1$, and that maximum efficiency occurs in the vicinity of $2c/f_1 = 0.25$. The maximum efficiency, obtained for the system with a 70^o-rim-angle paraboloid, is 71.3 percent. In this region of best performance, the rim angle of the primary reflector has a very small effect on the collection system efficiency. The maximum value of each curve represents the optimum exchange between obstruction and radiation losses for the double-reflector system with the specified paraboloid.

At $2c/f_1 = 1$, where the receiver is positioned behind the primary reflector, the collection system efficiency is appreciably lower than the maximum value shown at $2c/f_1 = 0.25$. In the calculation of collection system efficiency, the minimum receiver obscuration loss was assumed. A practical system will probably exhibit a larger obscuration and will, consequently, have a lower efficiency than the maximum shown. In a realistic situation, maximum efficiency will probably occur when $0.25 \leq 2c/f_1 \leq 1.0$.

Figure 5 shows the effect of axial displacement Δx of the hyperboloidal secondary reflector on the peak collection system efficiency. The peak collection system efficiency is plotted as a function of $2c/f_1$ for $\Delta x/f_1 = 0$, 0.00186, and 0.00372 and for a paraboloidal rim angle of 70^o. For every value of $2c/f_1$, the peak collection system efficiency

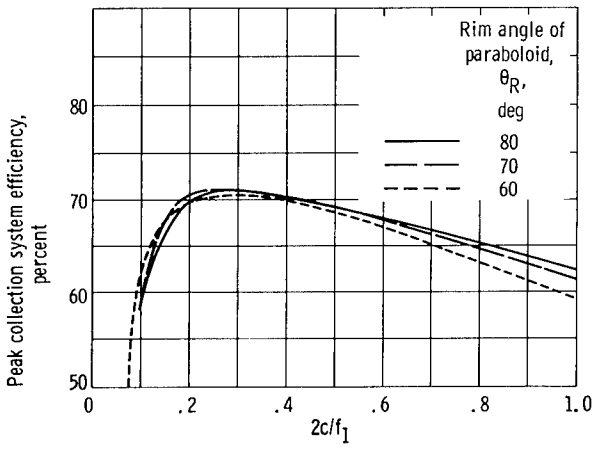

Figure 4. - Effect of paraboloidal reflector rim angle on peak efficiency of hyperboloidal double-reflector collection system.

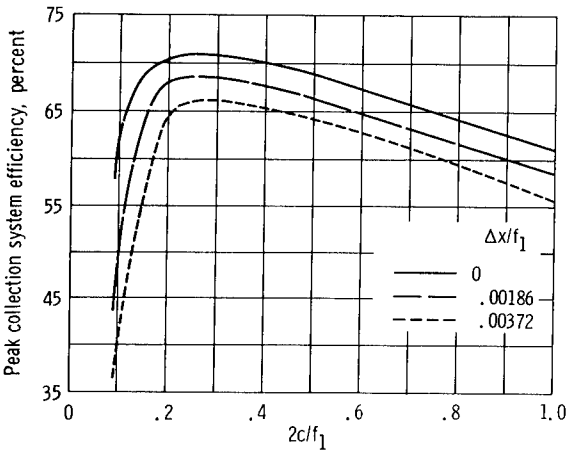

Figure 5. - Effect of hyperboloidal secondary reflector axial displacement on peak efficiency of double-reflector collection system. Rim angle of paraboloid, 70°.

decreases with increasing axial displacement. The reduction in efficiency is, on the average, approximately 1.35 efficiency points for a change of $\Delta x/f_1 = 0.001$. The chosen values of $\Delta x/f_1$ correspond to secondary reflector axial displacements of 0, 0.02, and 0.04 foot for a 70°-rim-angle paraboloidal reflector 30 feet in diameter.

Ellipsoidal Secondary Reflector

Figure 6(a) shows the efficiency of a double-reflector collection system with an ellipsoidal secondary reflector and a 60°-rim-angle paraboloid as a function of $D_s/2c$ for various values of $2c/f_1$. Also shown are lines of constant eccentricity.

For each value of $2c/f_1$, the collection system efficiency increases rapidly with growing values of $D_s/2c$ up to a maximum because of the increased concentration of energy, which reduces the receiver aperture diameter and, consequently, the radiation loss. After the maximum is reached, the simultaneously increasing obstruction losses of the secondary reflector predominate.

Patterns identical with those of figure 6(a) are illustrated in figures 6(b) and (c) for a double reflector system with paraboloids of 70° and 80° rim angles. The peak efficiencies from the curves in figure 6 are plotted in figure 7 as functions of $2c/f_1$ for the three paraboloid rim angles. The peak collection system efficiency increases with decreasing values of $2c/f_1$; it also improves with increasing rim angles for most of the range of $2c/f_1$. The maximum collection system efficiency of 70.5 percent occurred with the 80°-rim-angle paraboloid at $2c/f_1 \approx 0.25$.

With the receiver aperture located at the vertex of the paraboloid where $2c/f_1 = 1.0$, the peak collection system efficiency improves markedly with increasing rim angle but remains substantially lower than the maximum collection system efficiency, which occurs with the receiver aperture closer to the secondary reflector.

Figure 8 shows the effect of axial displacement Δx of the ellipsoidal secondary reflector on the peak collection system efficiency. The peak efficiency is plotted as a function of $2c/f_1$ for $\Delta x/f_1$ values of 0, 0.00225, and 0.0045 for a paraboloidal rim angle of 80°. For every value of $2c/f_1$, the peak collection system efficiency decreases with increasing axial displacement. The reduction in efficiency is, on the average, approximately 1.35 efficiency points for a change in $\Delta x/f_1$ of 0.001. The selected values of $\Delta x/f_1$ correspond to secondary reflector axial displacements of 0, 0.02, and 0.04 foot with an 80°-rim-angle paraboloidal reflector 30 feet in diameter.

The calculated values of r and D_s for the double-reflector system varied from 0.45 to 1.3 and from 0.5 to 22 feet, respectively.

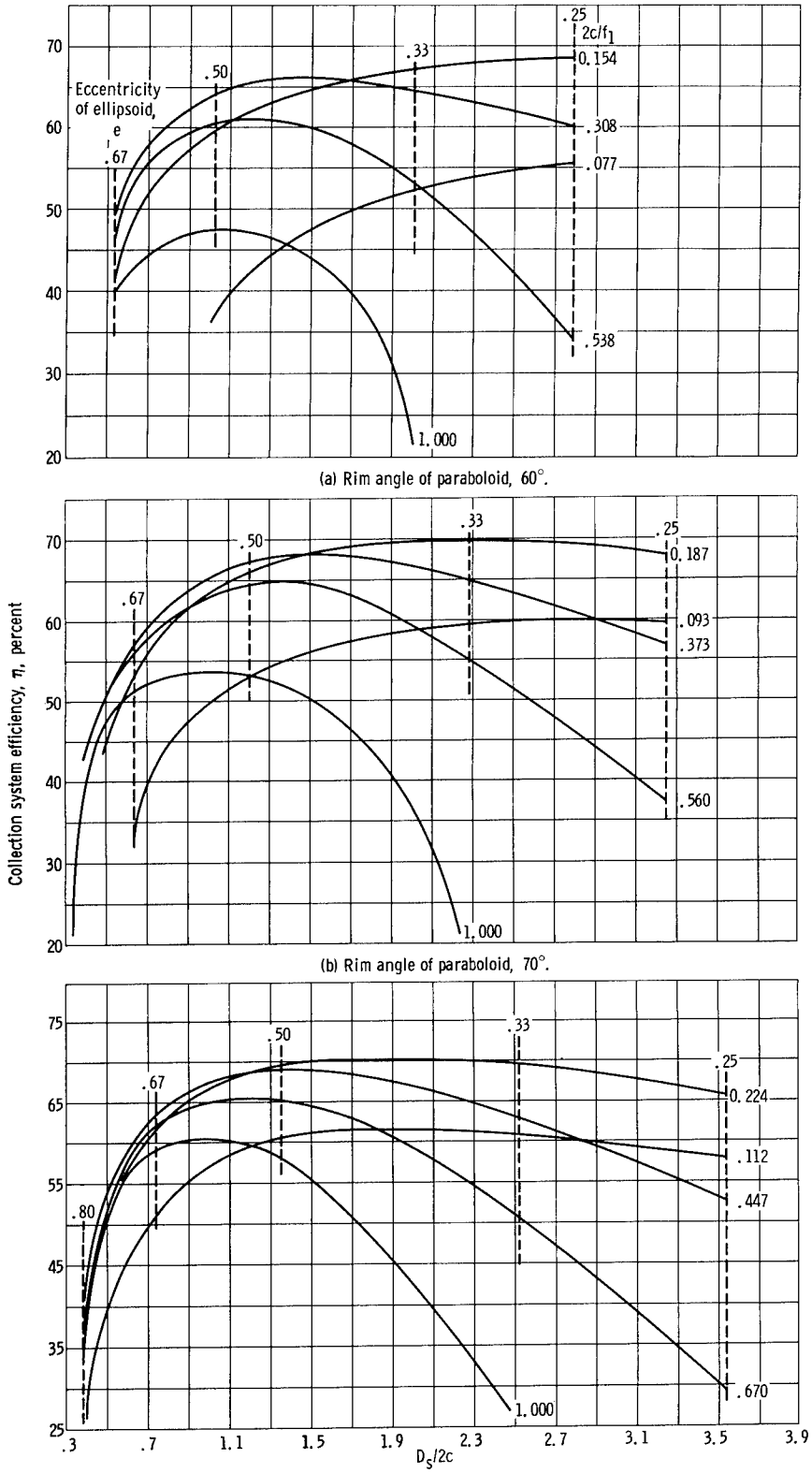

Figure 6. - Effect of ellipsoidal secondary reflector size and contour on efficiency of double-reflector collection system.

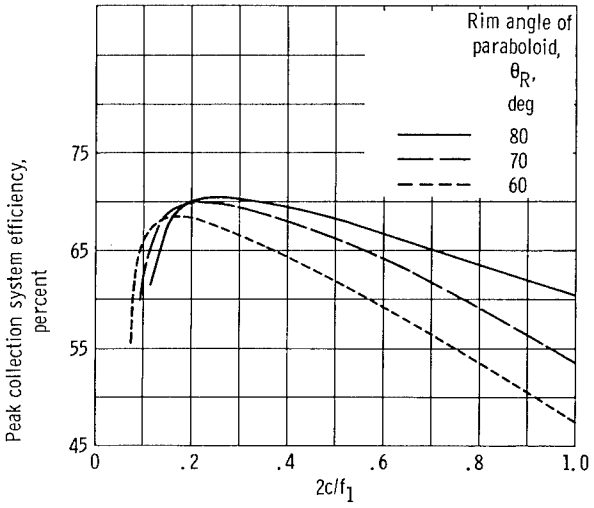

Figure 7. - Effect of paraboloidal reflector rim angle on peak efficiency of ellipsoidal double-reflector collection system.

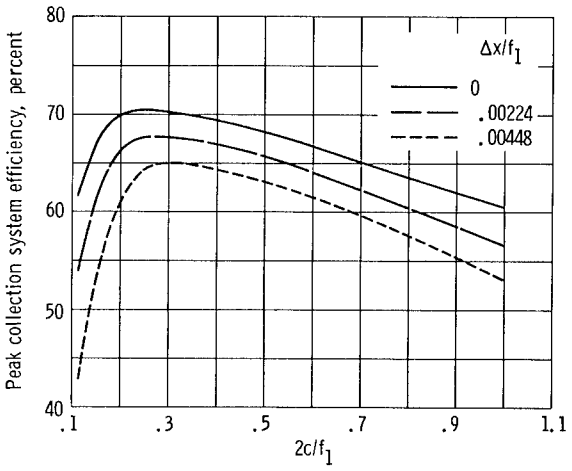

Figure 8. - Effect of ellipsoidal secondary reflector axial displacement on peak collection efficiency of double-reflector collection system. Rim angle of paraboloid, 80°.

Comparison With Single-Reflector Collection System

The collection system efficiency of a power system employing a single paraboloid of various rim angles with the cavity receiver aperture at the focus was calculated for comparison with a power system utilizing a double-reflector collection system.

It is postulated that the power conversion system components and supporting structure can be confined within the projection of the receiver when a single paraboloid is utilized and that the receiver obstruction factor can be limited to 3 percent of the incident energy.

The calculation of the collection system efficiency of a single-paraboloid power system is based on the assumption that the paraboloidal reflector has a maximum surface error of 15 minutes and a reflectivity of 0.9. Also, the receiver operating temperature is assumed at 2200° R. These conditions are identical to those employed in the calculation of the collection system efficiency of the double-reflector system. Collection system efficiency is plotted as a function of the paraboloidal reflector rim angle θ_R in figure 9. Changes in the reflector rim angle between 30° and 60° have relatively little effect on the collection system efficiency, which varies only 2 efficiency points for this range of rim angles; the efficiency maximizes when the rim angle is 45°.

The maximum collection system efficiency of the single-paraboloid system is approximately 81 percent as compared with a peak efficiency of approximately 71 percent for the double-reflector system with either the hyperboloidal or ellipsoidal secondary reflector. This difference in collection system efficiency is primarily due to the absorption loss on the second reflection associated with the double-reflector collection system.

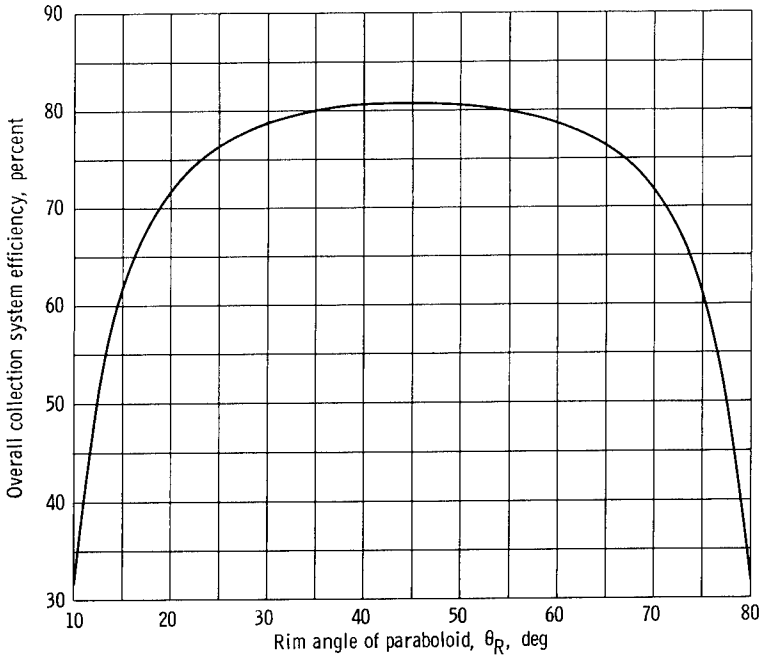

Figure 9. - Effect of paraboloidal reflector rim angle on efficiency of single-paraboloid-reflector collection system. Diameter of paraboloidal reflector, 30 feet; obstruction (fraction of incident energy), 0.03; reflectivity of reflector, 0.9; reflector surface error, 15 minutes; receiver operating temperature, 2200° R; receiver cavity assumed as blackbody.

A problem associated only with the double-reflector system is the effect of the concentration of solar energy upon the secondary reflector. This concentration of energy may result in an unacceptably high temperature for an optical surface. At the point of peak collection system efficiency, a ratio of primary reflector to secondary reflector area of approximately 60 to 1 exists. In the vicinity of the Earth where the solar flux is 130 watts per square foot, such a concentration of energy will result in a secondary reflector operating temperature of approximately 1100° R if the secondary reflector dissipates energy effectively from one side only with an emissivity of 1, and absorbs no direct solar radiation.

Operation of the collection system under this adverse condition may necessitate some means of cooling the secondary reflector; this requirement will impose a need for a heat rejection system and an additional degree of complication.

Effect of Receiver Operating Temperature

The effect of receiver operating temperature on the collection system efficiency was determined for both the double-reflector and the single-paraboloid collection system. As the receiver operating temperature was varied from 2200° to 3000° R, the maximum col-

lection system efficiency of the single-paraboloid system dropped from 81 to 65 percent, while the maximum efficiency of the double-reflector collection system dropped from 71 to 51 percent. The larger reduction in the double-reflector collection system efficiency with increasing temperature is due to the slightly larger receiver aperture diameter, which produces a larger radiation loss.

SUMMARY OF RESULTS

A double-reflector solar collection system was analytically surveyed with regard to its collection efficiency to provide an evaluation of its applicability to a solar dynamic power system. The results of the study are as follows:

1. Under the most optimistic conditions, the collection system efficiency of a power system comprising a double-reflector system with either a hyperboloidal or ellipsoidal secondary reflector is lower than the efficiency of a system with a single reflector. The maximum efficiency of the double-reflector system is approximately 71 percent as compared with 81 percent for the system with the single-paraboloidal reflector. The lower collection system efficiency is primarily due to the absorption loss associated with the second reflection in the double-reflector collection system.

2. The maximum collection system efficiency for either double-reflector system showed only a slight sensitivity to paraboloidal rim angle. The variation in maximum efficiency was less than 2 points for the range of paraboloidal rim angles from 60° to 80°.

3. The efficiency of either double-reflector collection system is sensitive to the accuracy of positioning the secondary reflector. A secondary reflector displacement Δx corresponding to a $\Delta x/f_1$ value of 0.001 deteriorates the collection system efficiency by 1.35 efficiency points.

4. The concentration of energy on the secondary reflector in a double-reflector system may result in an unacceptably high temperature for an optical surface. At the points of peak collection system efficiency, the secondary reflector temperature of a collection system operating in the vicinity of the Earth is approximately 1100° R, if it is assumed that the secondary reflector dissipates energy effectively from one side only with an emissivity of 1 and absorbs no direct solar radiation. The reflectivity of the reflector was considered to be 0.9. Operation of the collection system under this condition may necessitate the cooling of the secondary collector and ultimately may require a heat rejection system.

Lewis Research Center,
National Aeronautics and Space Administration,
Cleveland, Ohio, April 5, 1966.

APPENDIX A

DETERMINATION OF COLLECTION SYSTEM EFFICIENCY FOR DOUBLE-REFLECTOR COLLECTION SYSTEM

The collection system efficiency defines the ratio of the energy available to a thermodynamic cycle to that which is available as incident solar energy. The energy available to the cycle is that retained by the receiver. Therefore, the collection system efficiency is given by the following expression:

$$\text{collection system efficiency} = \frac{\text{net energy into receiver}}{\text{incident solar energy}}$$

$$\eta = \frac{E_a - E_r}{E_i} \tag{A1}$$

The incident solar energy is that which is intercepted by the projected area of the primary paraboloid reflector; that is,

$$E_i = \frac{\pi D_p^2 S}{4} \tag{A2}$$

The energy into the receiver is that available after obstruction and absorption losses have been incurred.

The energy available after obstruction is

$$S\left(\frac{\pi D_p^2}{4} - \frac{\pi D_x^2}{4}\right) = \frac{\pi}{4} S\left(D_p^2 - D_x^2\right) \tag{A3}$$

where D_x is the diameter of the primary reflector from which energy is obstructed by either the secondary reflector or the receiver aperture. The larger value of D_x is employed.

The energy remaining after absorption of energy by the two reflectors in the system is

$$\frac{\pi}{4} S\left(D_p^2 - D_x^2\right)\rho^2$$

where ρ is the reflectivity of the reflectors. The energy absorbed by the receiver is

$$E_a = \frac{\pi}{4} S \left(D_p^2 - D_x^2\right) \rho^2 \alpha$$

where α is the effective absorptivity of the receiver to solar radiation. The energy loss from the receiver by radiation is

$$E_r = \epsilon \sigma \pi r^2 T^4 \tag{A4}$$

Substituting equations (A2), (A3), and (A4) into equation (A1) results in the following:

$$\eta = \frac{\frac{S}{4}\left(D_p^2 - D_x^2\right)\rho^2\alpha - \epsilon\sigma r^2 T^4}{\frac{D_p^2}{4} S} \tag{A5}$$

The diameter of the primary reflector obstructed by the secondary reflector is

$$D_s = \frac{2(e^2 - 1)a \sin \theta_R}{1 + e \cos \theta_R} \qquad \text{(for hyperboloid)} \tag{A6}$$

$$D_s = \frac{2(1 - e^2)a \sin \theta_R}{1 - e \cos \theta_R} \qquad \text{(for ellipsoid)} \tag{A7}$$

The diameter of the primary reflector obstructed by the receiver (the diameter subtended by the receiver aperture from the focus of the paraboloid) is

$$D_r = 2k \sin\left(\arctan \frac{r}{2c}\right)$$

$$= \frac{2(2f_1)\sin\left(\arctan \frac{r}{2c}\right)}{1 + \cos\left(\arctan \frac{r}{2c}\right)} \tag{A8}$$

Either D_s or D_r, whichever is larger, is substituted for D_x in equation (A5). The diameters D_s and D_r are illustrated in figure 2 (p. 8).

APPENDIX B

DETERMINATION OF DIAMETER OF RECEIVER APERTURE IN DOUBLE-REFLECTOR COLLECTION SYSTEM

The location of solar energy reflected from a double-reflector system is determined by a ray analysis, and the receiver aperture diameter is sized to accommodate the ray with the maximum displacement.

The combination of reflectors employed is a paraboloid as the primary reflector and a hyperboloid or ellipsoid as the secondary reflector. See figure 1 (p. 2) for the configurations and the system arrangement.

The bases for the calculation of the receiver aperture size are as follows:

(1) The angle of incidence of a ray is equal to the angle of reflection.

(2) The focus of the secondary reflector is coincident with the focus of the primary reflector.

(3) The receiver aperture is located at the second focus of the secondary reflector.

The equation of the hyperboloidal secondary reflector is

$$\frac{x^2}{a^2} - \frac{y^2}{b^2} = 1 \tag{B1}$$

Similarly, if the secondary reflector is an ellipsoid, the equation is

$$\frac{x^2}{a^2} + \frac{y^2}{b^2} = 1 \tag{B2}$$

The path of a solar ray collected by a hyperboloidal double-reflector system is shown in figure 10. When the optic axis of the collection system is aimed at the center of the Sun, solar energy is received at the primary paraboloid over an angle of $\pm\beta$ with regard to this axis. The total subtended angle 2β of the solar disk is equal to 32 minutes in the vicinity of Earth.

The point on the primary reflector from which the incident energy is reflected is designated by the angle θ. This is the angle subtended from the focal point F by a given spot on the paraboloid and the optic axis. A ray incident to the paraboloid with an angle β in respect to the optic axis and striking the paraboloid at a position θ where the angular surface error is δ_1 will be reflected to form an angle $(\theta + \beta + 2\delta_1)$ with the optic axis. This ray will impinge on the secondary reflector to be reflected with an angle φ

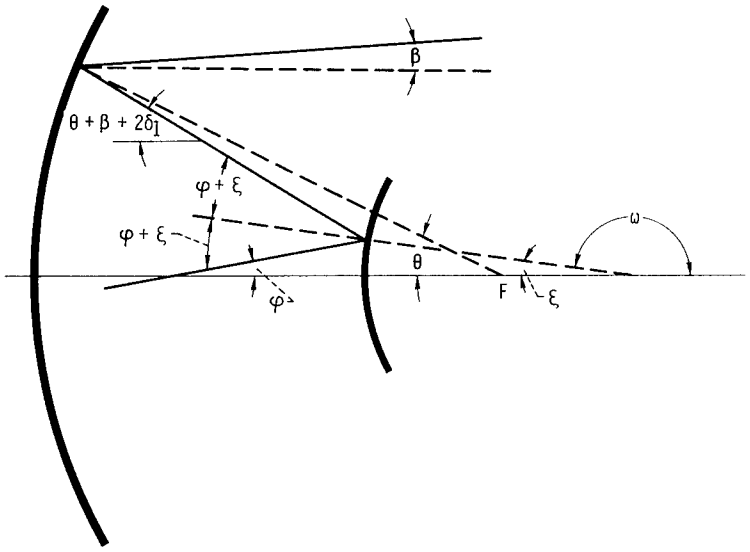

Figure 10. - Ray-trace diagram of hyperboloidal double-reflector solar collection system.

in respect to the optic axis. The angular surface error of the secondary reflector will be introduced later in the development of the equation. The ray will then be intercepted by the plane of the receiver aperture, which is perpendicular to the optic axis, at a radius R from this axis. The distance R is given by the following expression:

$$R = (x + c)\tan \varphi - y \tag{B3}$$

where x and y are the coordinates of the secondary reflector from which a given ray is reflected.

To determine the angle φ of the ray reflected from the secondary reflector, it is necessary to define the direction from which the ray arrives and the point at which it is intercepted by the secondary reflector. A ray arriving at the secondary reflector by reflection from the primary reflector has the equation

$$y = m_{rp}x + d \tag{B4}$$

To determine the point of intersection of this ray with the secondary reflector, equation (B4) must be solved simultaneously with equation (B1) or (B2) where the respective secondary reflector is a hyperboloid or an ellipsoid.

When the secondary reflector is a hyperboloid, substitution of equation (B4) into equation (B1) results in the following equation:

$$\left(b^2 - a^2m_{rp}^2\right)x^2 - \left(2a^2dm_{rp}\right)x - a^2d^2 - a^2b^2 = 0 \tag{B5}$$

Solving for x directly in terms of a, b, d, and m_{rp} yields

$$x = \frac{a^2 d m_{rp} \pm ab\sqrt{d^2 + b^2 - a^2 m_{rp}^2}}{b^2 - a^2 m_{rp}^2} \tag{B6}$$

The solution for y is

$$y = \pm \frac{b}{a}\sqrt{x^2 - a^2} \tag{B7}$$

The solution for x requires the designation of the four parameters a, b, d, and m_{rp}. The values of d and m_{rp} are derived in appendix C. For the hyperbola, the values of a and b are related as follows:

$$b^2 = a^2(e^2 - 1) = \frac{c^2}{e^2}(e^2 - 1) \tag{B8}$$

Consequently, the specification of c and e as variables will establish the required values of a and b.

The geometry of figure 10 indicates that

$$\varphi = (\theta + \beta + 2\delta_1) - 2\xi \tag{B9}$$

and that

$$\xi = 180 - \omega$$

or that

$$\tan \xi = \tan(180 - \omega) = - \tan \omega \tag{B10}$$

where ω is the angle of the normal to the secondary collector measured counterclockwise from the optic axis.

When the secondary reflector has an angular error of $\pm\delta_2$, the angle of the normal ω to the secondary varies by $\pm\delta_2$ and the angle ξ varies equally by $\pm\delta_2$; therefore, equation (B9) becomes

$$\varphi = (\theta + \beta + 2\delta_1) - 2(\xi \pm \delta_2) \tag{B11}$$

The value of $-\delta_2$ is employed in equation (B11) to provide the largest value of φ which is consistent with obtaining the maximum displacement of the ray. The slope of the normal to the hyperbola, tan ω, is equal to the negative reciprocal of the slope of the tangent to the hyperbola. Thus,

$$\tan \omega = \frac{-1}{m_{th}} \tag{B12}$$

The slope of the tangent to the hyperbola is the first derivative of equation (B1) as follows:

$$m_{th} = \left(\frac{dy}{dx}\right) = \frac{b^2 x}{a^2 y} \tag{B13}$$

Substituting equation (B13) into equation (B12) yields the expression for the slope of the normal to the hyperboloid, which is

$$\tan \omega = - \frac{a^2 y}{b^2 x} \tag{B14}$$

If equation (B14) is substituted into equation (B10), the result is

$$\tan \xi = \frac{a^2 y}{b^2 x}$$

and

$$\xi = \text{arc tan} \frac{a^2 y}{b^2 x} \tag{B15}$$

Substituting equation (B15) into equation (B11) yields

$$\varphi = (\theta + \beta + 2\delta_1) - 2\left(\text{arc tan} \frac{a^2 y}{b^2 x} \pm \delta_2\right) \tag{B16}$$

The receiver aperture is sized to capture all the energy reflected from the double-

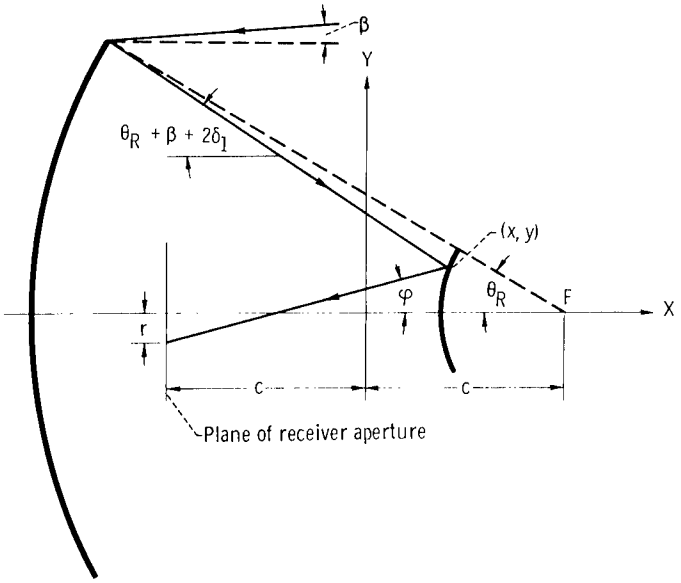

Figure 11. - Parameters of collection system with hyperboloidal secondary reflector.

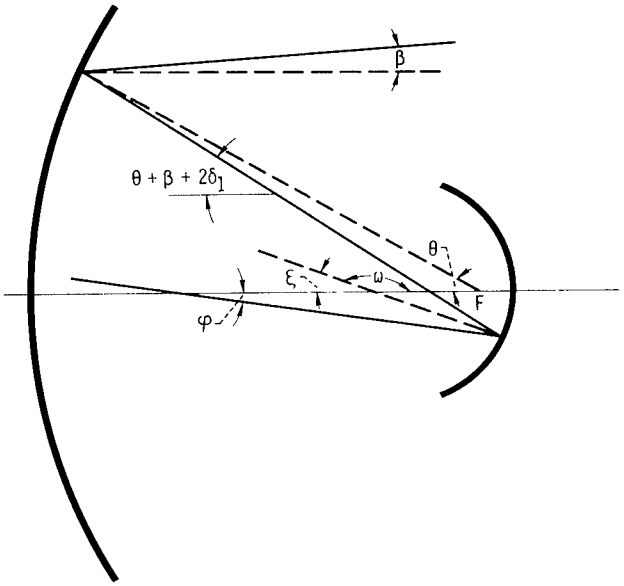

Figure 12. - Ray-trace diagram of ellipsoidal double-reflector solar collection system.

reflector system. As shown in figure 11, the receiver aperture radius r necessary to accommodate this condition is determined by the position at which the ray with the maximum deflection is intercepted by the plane of the receiver aperture. This ray is reflected from the rim of the paraboloid where the angle $\theta = \theta_R$. The value of r in accordance with equation (B3) is

$$r = (x + c)\tan \varphi - y$$

where φ is given by equation (B16).

The path of solar rays collected by an ellipsoidal double-reflector system is shown in figure 12. The procedure for determining the location of rays after reflection from the secondary reflector is the same as that for the hyperboloid. When the secondary reflector is an ellipsoid, equations (B2) and (B4) are solved simultaneously for the point of intersection with the secondary reflector of a ray reflected from the primary reflector. The resulting equation is

$$\left(b^2 + a^2 m_{rp}^2\right)x^2 + 2a^2 d m_{rp} x + a^2 d^2 - a^2 b^2 = 0 \qquad \text{(B17)}$$

Solving for x yields

$$x = \frac{-a^2 d m_{rp} \pm ab\sqrt{a^2 m_{rp}^2 + b^2 - d^2}}{b^2 + a^2 m_{rp}^2} \tag{B18}$$

and solving for y gives

$$y = \pm \frac{b}{a}\sqrt{a^2 - x^2} \tag{B19}$$

The parameters d and m_{rp} are described in appendix C. For the ellipse, the values of a and b are related in the following manner:

$$b^2 = a^2(1 - e^2) = \frac{c^2}{e^2}(1 - e^2) \tag{B20}$$

The specification of c and e as variables establishes the values of a and b.

The ray incident to the ellipsoidal secondary reflector is reflected with an angle φ in respect to the optic axis as shown in figure 12. This geometry indicates that

$$\varphi = -(\theta + \beta + 2\delta_1) + 2\xi \tag{B21}$$

and

$$\xi = 180 - \omega$$

or

$$\tan \xi = \tan(180 - \omega) = -\tan \omega \tag{B22}$$

When the secondary reflector has an angular surface error of $\pm\delta_2$, equation (B21) becomes

$$\varphi = -(\theta + \beta + 2\delta_1) + 2(\xi \pm \delta_2) \tag{B23}$$

The slope of the normal to the ellipsoid, $\tan \omega$, is

$$\tan \omega = -\frac{1}{\left(\frac{dy}{dx}\right)} \tag{B24}$$

The first derivative of equation (B2) is

$$\left(\frac{dy}{dx}\right) = -\frac{b^2x}{a^2y} \tag{B25}$$

Substituting equation (B25) into equation (B24) gives

$$\tan \omega = \frac{a^2y}{b^2x} \tag{B26}$$

If equation (B26) is substituted into equation (B22), the result is

$$\tan \xi = -\frac{a^2y}{b^2x}$$

and

$$\xi = \arctan -\frac{a^2y}{b^2x} \tag{B27}$$

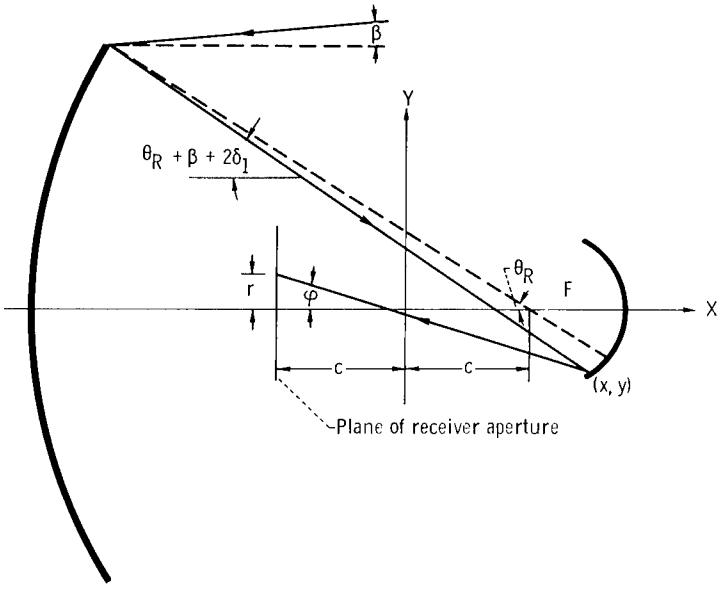

Figure 13. - Parameters of collection system with ellipsoidal secondary reflector.

Substituting equation (B27) into equation (B23) produces

$$\varphi = -(\theta + \beta + 2\delta_1) + 2\left[\arctan\left(-\frac{a^2y}{b^2x}\right) \pm \delta_2\right] \tag{B28}$$

The receiver aperture radius, as shown in figure 13, is given by the following expression:

$$r = (x + c)\tan \varphi - y$$

where φ is given by equation (B28).

APPENDIX C

DETERMINATION OF EQUATION OF PARAMETERS m_{rp} AND d OF RAY REFLECTED FROM PRIMARY PARABOLOID

The equation of a ray reflected from the surface of a paraboloid is

$$y = m_{rp}x + d \tag{C1}$$

When $x = 0$, $y = d$.

From figure 14 it is evident that

$$m_{rp} = - \tan(\theta + \beta + 2\delta_1)$$

and

$$d = x_3 \tan(\theta + \beta + 2\delta_1)$$

Therefore,

$$y = - x \tan(\theta + \beta + 2\delta_1) + x_3 \tan(\theta + \beta + 2\delta_1) \tag{C2}$$

Since $x_3 = c - (x_1 - x_2)$, $x_1 = y_a/\tan\theta$, and $x_2 = y_a/\tan(\theta + \beta + 2\delta_1)$, then

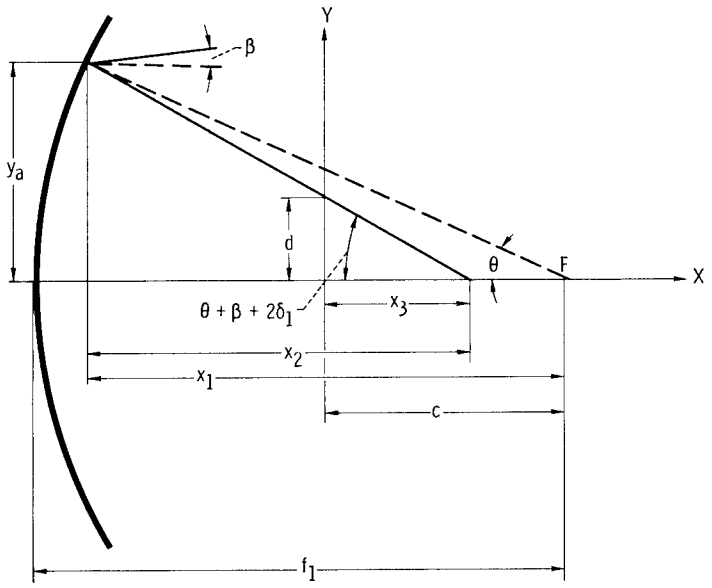

Figure 14. - Parameters of ray reflected from paraboloidal reflector.

$$x_3 = c - y_a\left[\frac{1}{\tan\theta} - \frac{1}{\tan(\theta + \beta + 2\delta_1)}\right] \tag{C3}$$

However, $y_a = k \sin\theta$, and

$$k = \frac{2f_1}{1 + \cos\theta} \tag{C4}$$

Therefore,

$$y_a = \frac{2f_1 \sin\theta}{1 + \cos\theta} \tag{C5}$$

and

$$x_3 = c - \frac{2f_1 \sin\theta}{1 + \cos\theta}\left[\frac{1}{\tan\theta} - \frac{1}{\tan(\theta + \beta + 2\delta_1)}\right] \tag{C6}$$

At the rim of the paraboloid, $y_a = D_p/2$ and $\theta = \theta_R$; therefore,

$$f_1 = \frac{D_p(1 + \cos\theta_R)}{4 \sin\theta_R} \tag{C7}$$

where D_p is the diameter of the primary paraboloid and θ_R is the rim angle of the paraboloid.

APPENDIX D

DETERMINATION OF EFFECT OF AXIAL DISPLACEMENT OF SECONDARY REFLECTOR ON DIRECTION OF REFLECTED RAY

When the secondary reflector is axially displaced, its focus is shifted from the focal point F of the paraboloid. This axial displacement, designated as Δx, is measured so that the reflectors are moved further apart. This direction is compatible with the ray considered in the analysis in appendix B to provide the largest displacement in the plane of the receiver aperture.

A solar ray reflected from the paraboloid is now intercepted by the secondary reflector at another location and thereby is reflected from the secondary with a change in direction φ which is due to the change in the angle of the normal ω at the point of intersection. As a result, the value of r is also altered.

To calculate the effect of Δx on the values of φ and r for the same reflector configuration, the coordinate axis is translated with the secondary reflector. Therefore, the same values of c and e define the same secondary reflector and leave the values of a and b unchanged. The ray from any given point on the paraboloidal reflector with the equation

$$y = m_{rp}x + d$$

has the same slope m_{rp}, but a different y-intercept d. The variation in the y-intercept d with a given variation in Δx is

$$\Delta d = \Delta x \tan(\theta + \beta + 2\delta_1)$$

and the new intercept d_a is

$$d_a = d - \Delta x \tan(\theta + \beta + 2\delta_1)$$

From knowledge of the parameters a, b, d_a, and m_{rp} associated with a given value of Δx, the point of intersection with the secondary reflector and the resulting values of φ and r can be determined as outlined in appendix B.

If the receiver position remains fixed while the secondary reflector is displaced a distance Δx, the distance between the secondary reflector and the receiver aperture increases from (x + c) to (x + Δx + c), and the corresponding value of r becomes

$$r = (x + \Delta x + c)\tan \varphi - y$$

"The aeronautical and space activities of the United States shall be conducted so as to contribute . . . to the expansion of human knowledge of phenomena in the atmosphere and space. The Administration shall provide for the widest practicable and appropriate dissemination of information concerning its activities and the results thereof."

—NATIONAL AERONAUTICS AND SPACE ACT OF 1958

NASA SCIENTIFIC AND TECHNICAL PUBLICATIONS

TECHNICAL REPORTS: Scientific and technical information considered important, complete, and a lasting contribution to existing knowledge.

TECHNICAL NOTES: Information less broad in scope but nevertheless of importance as a contribution to existing knowledge.

TECHNICAL MEMORANDUMS: Information receiving limited distribution because of preliminary data, security classification, or other reasons.

CONTRACTOR REPORTS: Technical information generated in connection with a NASA contract or grant and released under NASA auspices.

TECHNICAL TRANSLATIONS: Information published in a foreign language considered to merit NASA distribution in English.

TECHNICAL REPRINTS: Information derived from NASA activities and initially published in the form of journal articles.

SPECIAL PUBLICATIONS: Information derived from or of value to NASA activities but not necessarily reporting the results of individual NASA-programmed scientific efforts. Publications include conference proceedings, monographs, data compilations, handbooks, sourcebooks, and special bibliographies.

Details on the availability of these publications may be obtained from:

SCIENTIFIC AND TECHNICAL INFORMATION DIVISION

NATIONAL AERONAUTICS AND SPACE ADMINISTRATION

Washington, D.C. 20546